Dominant-Negative Suppression of Ca$_v$2.1 Currents by α$_1$2.1 Truncations Requires the Conserved Interaction Domain for β Subunits

Robert S. Raike, Ph.D.[1,2], **Holly B. Kordasiewicz, Ph.D.**[1], **Randall M. Thompson, B.S.**[1], and **Christopher M. Gomez, M.D., Ph.D.**[1,3]

[1]Departments of Neurology and Neuroscience, University of Minnesota, Minneapolis, MN 55455

Abstract

Episodic ataxia type 2 (EA2) is an autosomal dominant disorder arising from *CACNA1A* mutations, which commonly predict heterozygous expression of Ca$_v$2.1 calcium channels with truncated α$_1$2.1 pore subunits. We hypothesized that α$_1$2.1 truncations in EA2 exert dominant-negative effects on the function of wild-type subunits. Wild-type and truncated α$_1$2.1 subunits with fluorescent-protein tags were transiently co-expressed in cells stably expressing Ca$_v$ auxiliary β subunits, which facilitate α$_1$-subunit functional expression through high-affinity interactions with the alpha interaction domain (AID). Co-expression of wild-type subunits with truncations often resulted in severely reduced whole-cell currents compared to expression of wild-type subunits alone. Cellular image analyses revealed that current suppression was not due to reduced wild-type expression levels. Instead, the current suppression depended on truncations terminating distal to the AID. Moreover, only AID-bearing α$_1$2.1 proteins co-immunoprecipitated with Ca$_v$ β subunits. These results indicate that Ca$_v$ β subunits may play a prominent role in EA2 disease pathogenesis.

Keywords

CACNA1A; P/Q-type; channelopathy; cerebellum; stress; Ca$_v$ β subunit

INTRODUCTION

The dominantly-inherited paroxysmal disorder episodic ataxia type 2 (EA2) results from mutations in the *CACNA1A* gene, which encodes the pore-forming α$_1$2.1 subunit of Ca$_v$2.1 voltage-gated calcium channels (Ophoff et al., 1996). The Ca$_v$2.1 calcium channel subtype regulates neurotransmission throughout the nervous system, but is predominantly expressed within cerebellar Purkinje cells (Usowicz et al., 1992; Stea et al., 1994; Westenbroek et al., 1995). Not surprisingly, cerebellar dysfunction is the primary feature of EA2 attacks, as patients experience bouts of symptoms such as ataxia, migraine and vertigo, in response to

emotional, physical or pharmacological stressors (Ptacek, 1998; Jen, 2000; Jen et al., 2004). Although episodic neurological disorders can be characterized by a wide range of symptoms, including epileptic seizures, paroxysmal dyskinesias or periodic paralysis, many also arise from mutations within ion channel genes (Jen, 1999; Ptacek, 1999). Thus, studying the pathophysiological mechanisms of individual diseases such as EA2 may be useful in the development of treatment strategies for episodic channelopathy disorders in general.

Voltage-gated calcium or Ca_v channels regulate an array of physiological processes including muscle contraction, hormone secretion, neurotransmission, and gene expression. This diversity in function is mainly due to the expression of 10 genetically distinct α_1 subunit subtypes that may make up the calcium channel pore (Ertel et al., 2000; Catterall et al., 2005). However, high voltage-activated (HVA) Ca_v channels are also composed of at least two auxiliary subunits, β and $\alpha_2\delta$, which modulate channel kinetics (Singer et al., 1991; Arikkath and Campbell, 2003; Catterall et al., 2005). The auxiliary β subunits also play a crucial role in the functional expression of Ca_v channels. These non-membrane-spanning subunits promote translocation of α_1 subunits from the endoplasmic reticulum (ER) to the plasma membrane through a high affinity association with the alpha interaction domain, AID, which is evolutionarily conserved in all α_1 subunit subtypes (Pragnell et al., 1994; De Waard et al., 1996; Bichet et al., 2000).

Functional expression studies involving EA2 mutations have firmly established that non- or hypo-conductive $\alpha_1 2.1$ subunits cause the disorder (Guida et al., 2001; Jen et al., 2001; Jouvenceau et al., 2001; Wappl et al., 2002; Imbrici et al., 2004; Spacey et al., 2004; Imbrici et al., 2005; Wan et al., 2005b; Jeng et al., 2006), which is largely but not exclusively associated with expression of $\alpha_1 2.1$ truncation mutants (Ophoff et al., 1996; Yue et al., 1998; Battistini et al., 1999; Denier et al., 1999; Jen et al., 1999; Denier et al., 2001; van den Maagdenberg et al., 2002; Wappl et al., 2002; Subramony et al., 2003; Jen et al., 2004; Mantuano et al., 2004; Eunson et al., 2005; Spacey et al., 2005; Wan et al., 2005a; Wan et al., 2005b; Scoggan et al., 2006). However, the molecular mechanisms by which non-functional $\alpha_1 2.1$ pores generate disease in EA2 are still debated. Although some studies have suggested that the loss of channel function in EA2 simply induces a haplo-insufficiency of $Ca_v 2.1$ currents (Wappl et al., 2002; Imbrici et al., 2004; Imbrici et al., 2005), substantial evidence argues that non-conductive $\alpha_1 2.1$ mutants in EA2 actually suppress the functional contributions of $Ca_v 2.1$ channels composed of wild-type subunits through a dominant-negative mechanism (Jouvenceau et al., 2001; Raghib et al., 2001; Arikkath et al., 2002; Page et al., 2004; Jeng et al., 2006). Studies have suggested that impaired translation or stability of wild-type $\alpha_1 2.1$ subunits contributes to EA2 pathogenesis (Raghib et al., 2001; Page et al., 2004), while other evidence implicates the interactions between non-conductive $\alpha_1 2.1$ mutants and auxiliary β subunits in the dominant-negative suppression of wild-type $\alpha_1 2.1$ subunit function (Arikkath et al., 2002; Jeng et al., 2006).

The lack of a clear disease model for EA2 may be due in part to important differences between methods of Ca_v channel functional expression in the laboratory. Therefore, to further test the hypothesis that $\alpha_1 2.1$ mutants in EA2 exert dominant-negative effects on $Ca_v 2.1$ function, we utilized a strategy designed to reliably record whole-cell $Ca_v 2.1$ currents from channels composed of auxiliary β and $\alpha_2\delta$ subunits and mixed populations of $\alpha_1 2.1$ subunits, containing both wild-type isoforms and truncation mutants. We found that non-conductive $\alpha_1 2.1$ truncations, including those associated with EA2, severely suppressed $Ca_v 2.1$ currents when co-expressed with wild-type $\alpha_1 2.1$ subunits. Current suppression was observed despite abundant expression of wild-type $\alpha_1 2.1$ subunits, demonstrating that these effects were not due to wild-type protein instability. Furthermore, of the several $\alpha_1 2.1$ truncation mutants tested, only those terminating distal to the AID suppressed $Ca_v 2.1$

currents. These results are consistent with a dominant-negative model of EA2 disease pathogenesis and further implicate the involvement of Ca_v β auxiliary subunits in EA2 pathophysiology.

METHODS

Design of full-length and truncated α₁2.1 subunit cDNAs

Single nucleotide mutations were engineered using the Quickchange mutagenesis PCR method (Stratagene, Cedar Creek, TX) and verified by nucleotide sequence analysis. Wild-type $\alpha_1 2.1$ subunits N-terminally tagged with cyan or yellow fluorescent protein (CFP-Wt or YFP-Wt) were generated by subcloning an 8 kb Bgl II/BamH I fragment containing a rabbit-human $\alpha_1 2.1$ subunit chimeric cDNA (Restituito et al., 2000) into the pECFP or pEYFP cloning vectors (Clontech, Paulo Alto, CA). As described previously (Restituito et al., 2000), this chimeric $\alpha_1 2.1$ cDNA encodes the rabbit brain BI-1 isoform (Genbank accession # X57476) fused to the human $\alpha_1 2.1$ extended C-terminus, which was cloned from human cerebellum. This full-length $\alpha_1 2.1$ chimeric cDNA clone translates proteins bearing 93% identity to the full-length human clone AF004884. The EA2 mutation 1443X (Denier et al., 1999) was generated by inserting a point mutation into the YFP-Wt construct using forward primer CGAGTTTCAC<u>TAG</u>GACAACGTGCTGTGG and reverse primer CCACAGCACGTTGTCCTAGTGAAACTCG. The 612X mutation, similar to a reported EA2 mutation (van den Maagdenberg et al., 2002) was generated by sublconing a 1.8 kb Bgl II/Sca I digested fragment from the full-length $\alpha_1 2.1$ cDNA into the pEYFP cloning vector. Point mutations were introduced into this construct to express $\alpha_1 2.1$ subunits truncated proximal (384X) and distal (402X) to the reported alpha interaction domain, AID (Pragnell et al., 1994), using forward and reverse primers GAAGCTGCGGCGG<u>TAG</u>CAGCAGATTG and CAATCTGCTGCTACCGCCGCAGCTTC, respectively for YFP-384X, and GGTGATCCTCGCA<u>TAG</u>GACGAGAGACCGACG and CGTCGGTCTCGTCCTATGCGAGGATCACC for YFP-402X. The 330X mutation (Subramony et al., 2003) was constructed via subcloning a BssH1 (site 1282) BamH1 fragment of the full-length $\alpha_1 2.1$ cDNA into the pEYFP cloning vector.

Cell culture

β_1-HEK cells (Rock et al., 1989; Piedras-Renteria et al., 2001; Barrett et al., 2005; Cao et al., 2005), which stably express human β_{1c} (Genbank accession # U86960; personal communication, Erika Piedras-Renteria, Loyola University, Chicago) and rabbit $\alpha_2\delta$ subunits (Genbank accession # M21948; Rock et al., 1989) were grown in low-calcium DMEM/F12 media (10% fetal bovine serum, 1% L-glutamine, 0.05% Gentamicin, 1% non-essential amino acids) and transfected with equimolar amounts of wild-type and mutant $\alpha_1 2.1$ subunit cDNAs using Lipofectamine (Invitrogen, Carlsbad, CA). Cells were plated onto poly-D lysine coated cover slips at low-density approximately 48 hrs post-transfection and recorded or imaged 2–4 hours later.

Electrophysiology

Whole-cell barium currents were recorded and captured using the patch-clamp technique with an Axopatch 200B amplifier, Digidata 1320A converter, and pCLAMP6 software (Axon instruments, Foster City, CA). Borosilicate micropipettes of 2–4 MΩ resistance were filled with (in mM): 125 CsCl, 5 EDTA, 2 MgCl₂, and 5 Glucose (pH 7.2 with CsOH and 275 mOsm with glucose). The recording solution was (in mM): 2.5 BaCl₂, 10 HEPES, 110 TEACl, and 30 TEAOH (pH 7.4 with methane sulfonic acid and 300 mOsm with glucose). Cells were viewed at 60x under oil immersion, on an Axiovert S100TV inverted microscope (Zeiss, Jena, Germany), and with CFP and YFP excitation/emission epifluorescence filter

sets (Chroma Technology, Rockingham VT). Cells were clamped at −80 mV, and recordings initiated after compensating for capacity transients and series resistance (70%). Linear leak was subtracted using the P/4 method and current records filtered using a 5kHz low-pass Bessel filter. Currents were evoked using 150 ms voltage steps from −60 to 60 mV at intervals of 10 seconds. Peak current density (Peak J, pA pF^{-1}) was measured at 0 mV. Whole-cell current density data for individual cells were fitted with the modified Boltzmann equation: Peak J = G $(V-V_{rev})[1 + exp (V_{0.5}-V)^{-k}]^{-1}$ to compare $Ca_v2.1$ channel open probability, where G = relative conductance, V = voltage, V_{rev} = reversal potential, $V_{0.5}$ = the voltage of half maximal activation, and k = the slope factor. Rates of activation and inactivation were measured from raw whole-cell current traces at 0, 10, and 20 mV step pulses, with I_{peak} = the time to reach the peak current and I_{r50} = the % peak current remaining at 50 ms. To control for wild type or mutant isoform expression level bias, dual-fluorescing cells were randomly selected for physiological recordings. To control for potential changes in the β_1-HEK cell line following several passages during this study, recordings of control cells transfected with CFP-Wt constructs were obtained throughout for each transfection. Recordings from control cells resulted in robust currents in each case. Only cells surviving through the entire I/V experiment and expressing detectable levels of currents were used for kinetic measurements.

Fluorescence microscopy

Images of randomly-selected β_1-HEK cells expressing CFP-tagged wild-type $\alpha_1 2.1$ subunits and YFP-tagged truncations were captured using an Olympus 1X70 inverted light microscope (Melville, NY) equipped with a Spot RT digital camera (Diagnostic Instruments, Sterling Heights, MI). Cells were treated identically to those used for electrophysiological experiments. Average CFP and YFP pixel intensities of several samples from individual cells imaged during the same sitting were calculated and analyzed following background subtraction using the MetaMorph acquisition and analysis software package (Molecular Devices Corporation, Sunnyvale, CA). Values expressed represent mean relative fluorescence intensities for each group of cells.

Immunoblot and immunoprecipitation

Immunoprecipitation and western blot experiments were performed essentially as previously reported (Restituito et al., 2000). Due to the availability of high quality commercial β_3 subtype-specific antisera (Alomone Labs, Israel), co-immunoprecipitation studies were carried out in β_3-HEK cells stably expressing rat β_3 and $\alpha_2\delta$ subunits (Kordasiewicz et al., 2006). Briefly, approximately 48 hours post-transfection, HEK cells stably expressing β_3 and $\alpha_2\delta$ subunits (β_3-HEK) were lysed with ice-cold buffer (M-PER; Pierce Biotechnology, Rockford, IL) supplemented with 10mM EDTA, 10mM EGTA and protease inhibitors (Complete Mini EDTA-free; Roche, Indianapolis, IN). For western blots, 30 µg of total lysate were subjected to SDS-PAGE on 8% tris-glycine gels (Invitrogen, Carlsbad, CA). Immunoprecipitation was performed by incubating 40 µL of staphylococcus protein A agarose beads (SPA; Invitrogen) with 5 µg of monoclonal anti-GFP (Roche) and 100 µg lysate. To remove unbound proteins, preparations were washed with TBS containing 1% Tween-20 (TBS-t) and then with TBS-t containing 10 mM tris base. Bound proteins were freed from SPA beads by boiling and denaturing followed by SDS-PAGE. For all immunoblots, proteins were transferred to nitrocellulose membranes, which were incubated with monoclonal anti-GFP (western blot) or polyclonal anti-β_3 (immunoprecipitation) and species-specific secondary antibodies. Chemiluminescent signals were developed using the ECL western detection kit (Roche).

Statistical analysis

Data expressed as means ± SEM and were statistically analyzed with ANOVA and a *post hoc* Bonferroni correction using a statistical software package (Statview, SAS Institute).

RESULTS

Truncated $\alpha_1 2.1$ subunits suppress $Ca_V 2.1$ currents in a length-dependent fashion

To directly test for a dominant-negative effect of truncated $\alpha_1 2.1$ subunits on $Ca_V 2.1$ channel function, we assembled a series of cDNA constructs designed to express wild-type and truncated $\alpha_1 2.1$ subunits, N-terminally tagged with cyan or yellow fluorescent protein, respectively (CFP and YFP; Figure 1A) and *transiently* expressed them in human embryonic kidney cells *stably* expressing Ca_V β and $\alpha_2\delta$ auxiliary subunits (β_1-HEK cells; Piedras-Renteria et al., 2001). Untransfected β_1-HEK cells expressing only the Ca_V auxiliary subunits failed to exhibit currents at any potential (Figure 1B). In contrast, whole-cell currents from voltage-clamped β_1-HEK cells expressing CFP-fluorescing wild-type $\alpha_1 2.1$ subunits (CFP-Wt) were easily obtainable (Figure 1B, Figure 2), and exhibited a mean peak current density of -75.5 ± 7.9 pA pF^{-1} at 0 mV (n = 16; Table 1). Consistent with all previous reports, none of the YFP-tagged $\alpha_1 2.1$ truncations tested here conducted detectable $Ca_V 2.1$ currents (not shown).

In several cases, co-expression of wild-type and truncated $\alpha_1 2.1$ subunits resulted in significantly reduced whole-cell $Ca_V 2.1$ current densities. Interestingly, the density of currents in co-transfected cells depended on the length of truncated isoform co-expressed. Co-expression of CFP-Wt subunits with either of the YFP-612X or YFP-1443X truncations, similar to mutants predicted from two distinct nonsense mutations associated with EA2 (Denier et al., 1999; van den Maagdenberg et al., 2002), resulted in severe reductions in $Ca_V 2.1$ currents across all voltages compared to control (Figure 1B, Figure 2A). Cells exhibited mean peak current densities of -24.5 ± 3.9 (n = 12, p < 0.0001) and -27.8 ± 7.1 (n = 9, p < 0.001) pA pF^{-1} at 0 mV, when co-expressing CFP-Wt subunits with YFP-612X or YFP-1443X truncations, respectively (Table 1). In addition, co-expression of YFP-612X truncations caused a slight but statistically-significant hyperpolarizing shift in channel activation relative to control (Figure 2B, Table 1).

In contrast, currents from cells co-expressing YFP-330X truncations, which corresponds to one possible outcome of a *CACNA1A* splice-site mutation reported by our group (Subramony et al., 2003), were similar in appearance (Figure 1B) and magnitude (Table 1) to those obtained from control cells expressing CFP-Wt subunits alone, with a mean peak current density of 71.8 ± 12.8 pA pF^{-1} at 0 mV (n = 13, p > 0.5). There were no significant kinetic changes associated with co-expression of YFP-330X truncations (Table 1, Figure 2). The lack of effects associated with YFP-330X co-expression indicates that the reported *CACNA1A* splice-site mutation may not encode an $\alpha_1 2.1$ truncation. Instead, recent studies propose that similar splice-site mutations associated with EA2 result in aberrantly-spliced $\alpha_1 2.1$ isoforms with unusual domain compositions (Eunson et al., 2005; Wan et al., 2005a). These results demonstrate that some but not all $\alpha_1 2.1$ truncations perturb $Ca_V 2.1$ function when co-expressed with wild-type subunits.

Dominant-negative $Ca_V 2.1$ current suppression by $\alpha_1 2.1$ truncations requires AID

We hypothesized that the inability of YFP-330X mutants to affect $Ca_V 2.1$ currents was related to their termination prior to the alpha interaction domain, AID, as all of the reported truncations associated with EA2 predict termination distal to its location (Denier et al., 1999; Jen et al., 1999; van den Maagdenberg et al., 2002; Jen et al., 2004). Membrane translocation and functional expression of Ca_V α_1 subunits depend on β subunit binding to

the AID, a 20 amino-acid sequence with 9 conserved residues, located within the α_1-subunit domain I–II cytoplasmic loop (Pragnell et al., 1994; Bichet et al., 2000). To determine if $\alpha_1 2.1$ truncations require the AID to suppress $Ca_v 2.1$ currents from wild-type subunits, we designed two additional cDNA constructs intended to express mutants terminating directly proximal (YFP-384X) or distal (YFP-402X) to the AID (Figure 1A). Co-expression of YFP-384X truncations with CFP-Wt subunits had no effect on the size of $Ca_v 2.1$ currents relative to control (Figure 1B, Figure 2A), resulting in a mean peak current density of -85.8 ± 11.2 pA pF^{-1} at 0 mV (n = 7, p > 0.1; Table 1). However, co-expression of YFP-402X truncations with CFP-Wt subunits caused severely reduced currents across all voltages (Figure 1B, Figure 2A), with a mean peak current density of 25.2 ± 5.9 pA pF^{-1} at 0 mV (n = 7, p < 0.001; Table 1), similar to the mean current densities following co-expression of the AID-bearing YFP-612X or YFP-1443X truncations. Therefore, co-expression of $\alpha_1 2.1$ truncations with wild-type subunits was associated with $Ca_v 2.1$ current densities which were suppressed to less than 40% of control exclusively when truncations contained the AID.

Co-expression of truncated isoforms does not result in wild-type protein instability

Findings from several other studies, including those reported here, indicate that mutant $\alpha_1 2.1$ subunits in EA2 likely inhibit the functional impact of wild-type subunits (Jouvenceau et al., 2001; Arikkath et al., 2002; Jeng et al., 2006). However, previous reports also suggest that $\alpha_1 2.1$ truncations could perturb $Ca_v 2.1$ currents by impairing translation or stability of wild-type subunits (Raghib et al., 2001; Page et al., 2004). Co-transfection of CFP-Wt and YFP-truncated $\alpha_1 2.1$ subunit constructs resulted in an abundance of cells with dual CFP and YFP fluorescence across all experiments, indicating ample expression of both the wild-type and mutant isoforms (Figure 3). Nevertheless, to rule out a link between the reduced $Ca_v 2.1$ current densities observed here and a decrease in wild-type $\alpha_1 2.1$ protein expression levels previously reported by others, we performed image analyses to compare the relative CFP fluorescence intensity (RF) individual β_1-HEK cells treated identically to those used for electrophysiological recordings. Compared to control cells expressing CFP-Wt subunits alone, there was no decrease in mean CFP fluorescence intensity detected in any of the groups co-expressing YFP-truncations (Table 2). In fact, mean CFP-Wt expression levels were remarkably similar across all groups, except for cells co-expressing YFP-1443X truncations, which actually exhibited significantly higher levels of CFP fluorescence intensity (69.2 ± 5.8 RF, n = 17) compared to control cells (50.1 ± 3.8 RF, n = 27; p < 0.005). These results clearly demonstrate that the reduction in whole-cell $Ca_v 2.1$ currents caused by co-expression of AID-bearing $\alpha_1 2.1$ truncations with wild-type subunits cannot be explained by a reduction of wild-type subunit translation or stability.

Truncation proximal to the AID prevents high-affinity Ca_v $\alpha_1 2.1$-β interactions

Although necessary for β subunit-mediated α_1 membrane translocation, the region of the AID is only one of several known to exhibit affinity for β subunit proteins (Pragnell et al., 1994; De Waard et al., 1996; Brice et al., 1997; Walker et al., 1998; Walker et al., 1999; Bichet et al., 2000; Cornet et al., 2002; Maltez et al., 2005). To examine the role of the AID in facilitating Ca_v α_1-β subunit associations, we tested preparations from HEK cells *stably* expressing $\beta 3$ and $\alpha_2 \delta$ auxiliary subunits (β_3-HEK) and *transiently* expressing YFP-384X, YFP-402X, or CFP-Wt $\alpha_1 2.1$ isoforms for the presence of $\alpha_1 2.1$-β proteins complexes. When immunoblotted with antisera to the $\alpha_1 2.1$ N-terminal fluorescent protein tag (anti-GFP), lysates from cells expressing β subunits and either the wild-type or mutant $\alpha_1 2.1$ proteins were positive for only the expected $\alpha_1 2.1$ reactive species (Figure 4A). Similarly, when these lysates were immunoblotted with anti-$\beta 3$ sera, a single approximately 60 kD species was detected, corresponding to the predicted β subunit molecular weight (Figure 4B, left panel). Anti-GFP did not react with lysates prepared from untransfected cells (Figure 4A, left and right panels) nor did anti-β 3 react with lysates prepared from HEK cells not

expressing β subunits (Figure 4B, left panel). To determine if the expressed $\alpha_1 2.1$ proteins form detectable complexes with β subunits, we first immunoprecipitated lysates from transfected cells with anti-GFP and staphylococcal protein A, and then transferred immunoprecipitates to membranes following SDS-PAGE separation. Anti-β3 antibody detected the same β subunit species in immunoprecipitates from cells expressing the CFP-Wt or YFP-402X $\alpha_1 2.1$ isoforms, but failed to yield detectable levels of the β subunit protein in preparations from cells expressing YFP-384X truncations, terminating proximal to the AID (Figure 4B, right panel). These data suggest that formation of these $\alpha_1 2.1$-β complexes is largely, if not exclusively, dependent on the amino acid residues contained within the AID, and further implicate α_1-β interactions in the suppression of $Ca_v 2.1$ currents we observed when wild-type $\alpha_1 2.1$ subunits and truncations terminating distal to the AID were co-expressed.

DISCUSSION

Episodic ataxia type 2 (EA2) is a paroxysmal ion channel disorder or channelopathy arising from one of several mutations within the *CACNA1A* gene, which encodes the pore-forming $\alpha_1 2.1$ subunit of $Ca_v 2.1$ channels (Ophoff et al., 1996). While attacks in patients with EA2 can be somewhat variable in character, it is not surprising that symptoms of cerebellar dysfunction are the predominant feature (Ptacek, 1999; Jen, 2000; Jen et al., 2004), given that cerebellar output through Purkinje cells relies heavily on the $Ca_v 2.1$ channel subtype (Swensen and Bean, 2003; Womack and Khodakhah, 2004; Walter et al., 2006). Study of the electrophysiological consequences of EA2 mutations has consistently demonstrated that the disorder is associated with a loss of $Ca_v 2.1$ channel function (Guida et al., 2001; Jen et al., 2001; Jouvenceau et al., 2001; Wappl et al., 2002; Imbrici et al., 2004; Spacey et al., 2004; Imbrici et al., 2005; Wan et al., 2005b; Jeng et al., 2006), but the implications for disease pathogenesis in EA2 are not so clear.

As previously reported for $\alpha_1 2.1$ subunits harboring EA2 mutations (Jouvenceau et al., 2001; Raghib et al., 2001; Arikkath et al., 2002; Page et al., 2004; Jeng et al., 2006), we routinely observed a dominant-negative suppression of $Ca_v 2.1$ channel currents when non-conductive $\alpha_1 2.1$ truncations were co-expressed with wild-type subunits. In the present study we also observed that these effects occurred despite abundant levels of wild-type subunit protein expression, adding to the growing evidence that non-conductive $\alpha_1 2.1$ mutants in EA2 exert dominant-negative effects on the functional impact rather than on the translation or stability of wild-type subunits (Jouvenceau et al., 2001; Raghib et al., 2001; Arikkath et al., 2002; Page et al., 2004; Jeng et al., 2006). The electrophysiological data presented here are novel in that only a subset of the truncated $\alpha_1 2.1$ isoforms tested suppressed currents from $Ca_v 2.1$ channels which were composed of wild-type subunits. Current suppression by truncations depended on whether or not they terminated distal to the AID, implying that $\alpha_1 2.1$ subunit interactions with auxiliary β subunits were crucial for the effect. This conclusion is supported by our demonstration that $\alpha_1 2.1$-β subunit heterodimers were detectable by immunoprecipitation only in samples with full-length or truncated $\alpha_1 2.1$ proteins bearing the AID, which agrees with several previous studies characterizing the role of the AID in the $\alpha_1 2.1$-β high-affinity interaction (Pragnell et al., 1994; De Waard et al., 1996; Brice et al., 1997; Walker et al., 1998; Walker et al., 1999; Bichet et al., 2000). Overall, our data suggest that AID-mediated interactions with β subunits permit truncated $\alpha_1 2.1$ subunits in EA2 to perturb the function of normal $Ca_v 2.1$ channels, a view consistent with the fact that all of the reported EA2 nonsense mutations predict $\alpha_1 2.1$ subunit truncations to terminate distal to the AID (Ophoff et al., 1996; Denier et al., 1999; van den Maagdenberg et al., 2002; Jen et al., 2004).

A model of EA2 pathophysiology involving Ca_v auxiliary β subunits is well supported by the literature. The functional density of Ca_v channels depends on the availability of auxiliary β subunits (Berrow et al., 1995; Gao et al., 1999), which in addition to normalizing channel activity (Lacerda et al., 1991) facilitate $α_1$ subunit membrane translocation by binding to the AID and masking several endoplasmic reticulum (ER) retention signals residing within the $α_1$ subunit domain I–II intracellular loop (Bichet et al., 2000; Cornet et al., 2002). Similar to our results, severely reduced Ca_v current densities have been observed *in situ* following exogenous expression of membrane-targeted peptides bearing the AID (Cuchillo-Ibanez et al., 2003). During the present study, we found no indication that expression of AID-bearing $α_1$2.1 truncations affected wild-type subunit expression levels. However, the suppression of Ca_v currents implies that the function of wild-type $α_1$2.1 subunits was reduced in $β_1$-HEK cells despite a stable pool of auxiliary β subunits. In agreement with this assessment, titration experiments performed by others show that the concentration of β subunits required to traffic $α_1$ subunits to the plasma membrane is substantially less than that required to modulate channel activity (Canti et al., 2001). Thus, $α_1$2.1 mutants in EA2 have the potential to sequester a significant portion of the available pool of β subunits, reducing the overall functional impact of Ca_v2.1 channels composed of wild-type $α_1$2.1 pores.

Nonetheless, the mechanisms of EA2 pathogenesis remain controversial due to several contradictory reports in the literature. Still under debate is whether EA2 arises from a simple haplo-insufficiency of wild-type Ca_v2.1 channels (Guida et al., 2001; Wappl et al., 2002; Imbrici et al., 2004), or if non-conductive $α_1$2.1 mutants cause disease by exerting dominant-negative effects on the function of Ca_v2.1 channels composed of wild-type subunits (Jouvenceau et al., 2001; Raghib et al., 2001; Page et al., 2004; Jeng et al., 2006). The discrepancies in the EA2 literature may be related to the differences in Ca_v channel heterologous expression systems and $α_1$2.1 isoforms employed by individual groups. As demonstrated by Jeng et al, $α_1$2.1 truncation mutants are more pathogenic when co-expressed with wild-type isoforms bearing extended C-termini, which are abundant in cerebellum (Restituito et al., 2000; Jeng et al., 2006; Kordasiewicz et al., 2006). We therefore devised a strategy to easily record whole-cell Ca_v2.1 currents from mammalian cells expressing a reliably mixed population of mutant and wild-type $α_1$2.1 pores by voltage-clamping cells stably expressing Ca_v auxiliary β and $α_2$δ subunits and co-transfected with fluorescent-tagged $α_1$2.1 subunit truncations and wild-type isoforms with extended C-termini.

Including the findings presented here, of the eight known studies where non- or hypo-conductive $α_1$ subunit mutants were co-expressed with wild-type subunits, six report a dominant-negative suppression of Ca_v currents (Jouvenceau et al., 2001; Raghib et al., 2001; Arikkath et al., 2002; Wappl et al., 2002; Imbrici et al., 2004; Page et al., 2004; Jeng et al., 2006). Moreover, of the five groups that describe current suppression, three, including our own, found evidence implicating Ca_v auxiliary β subunits in the EA2 disease process (Jouvenceau et al., 2001; Arikkath et al., 2002; Page et al., 2004; Jeng et al., 2006). Similar to the findings presented here, Arrikkath et al. used a cell line stably expressing $α_1$2.1 subunits and auxiliary β subunits to co-express a two-domain $α_1$2.1 truncation, and observed that the current-suppressing effects of the truncated isoform were completely abolished by mutations to amino acid residues within the AID that are critical for the high-affinity $α_1$-β interaction (Pragnell et al., 1994; De Waard et al., 1996; Arikkath et al., 2002). More recently, it was reported that the suppressive effects of EA2 truncations on exogenous Ca_v2.1 currents from wild-type $α_1$2.1 subunits were significantly alleviated by increasing the availability of β subunits (Jeng et al., 2006). However, the same approach failed to even modestly reverse the dominant-negative effects exerted by EA2 missense mutants (Jeng et al., 2006), which in addition to hypo-conduction exhibit defective intracellular trafficking

(Wan et al., 2005b). These latter findings suggest that α₁2.1 missense mutants may be more pathogenic than truncations.

While ample data argue for an EA2 model in which the disease process is facilitated by Ca_v auxiliary β subunits, the behavior of α₁2.1 mutants in neurons *in vivo* is presumably more complex than that suggested by studies performed in heterologous expression systems. Recently, Cao et al reported that exogenous over-expression of wild-type α₁2.1 subunits in neurons *in situ* increased Ca_v2.1 current density 5-fold without affecting synaptic transmission, while expression of non-conductive α₁2.1 mutants under the same conditions had no effect on the density of currents, but reduced the contribution of the endogenous Ca_v2.1 currents to the release of neurotransmitter (Cao et al., 2005; Cao and Tsien, 2005). These findings suggest that neurons, at least in culture, are able to functionally express α₁2.1 subunits much more densely than normal, but that expression of such a mixed population of wild-type subunits and non-conductive mutants causes dominant-negative defects in neurotransmission unrelated to whole-cell current density. Throughout the nervous system, synaptic transmission relies heavily on the activity of Ca_v2.1 channels, a reliance that can be a attributed in part to the targeted trafficking of α₁2.1 subunits to nerve terminals by Ca_v auxiliary β subunits (Wittemann et al., 200; Brice and Dolphin, 1999; Mochida et al., 2003a). However, Ca_v2.1 channel regulation of synaptic transmission also depends on the high-affinity interactions between the SNARE proteins of the synaptic release machinery and the synprint region of α₁2.1 subunits, located within the domain II–III cytoplasmic loop (Martin-Moutot et al., 1996; Mochida et al., 1996; Mochida et al., 2003b). Similar to the effects on Ca_v current density following the exogenous expression of membrane-targeted AID peptides (Cuchillo-Ibanez et al., 2003), synprint peptides exogenously expressed in neurons *in situ* cause a severe suppression of synaptic transmission (Mochida et al., 1996). Therefore, the results presented here and elsewhere suggest that the same protein-protein interactions which are crucial for α₁2.1 subunit trafficking and regulation of neurotransmission may also permit α₁2.1 mutants to act as decoys, entrapping a portion of the limited pool of regulatory proteins and decreasing the overall contributions of wild-type Ca_v2.1 currents to the maintenance of normal neuronal function.

Additional studies are needed to discern the discreet molecular events leading to a suppression of normal Ca_v2.1 function by mutant α₁2.1 subunits in neurons in EA2. Moreover, a detailed analysis of the kinetic consequences of wild type and truncated α₁2.1 subunit co-expression may uncover additional insights regarding the severity of the dysfunction. Furthermore, determining how a chronic reduction of Ca_v2.1 current magnitude triggers compensatory changes in calcium homeostasis will elucidate the etiology of the ataxic episodes in EA2. In turn, understanding the pathophysiology driving attacks in EA2 will have broader implications for a variety of other paroxysmal neurological disorders, including migraine, dystonia and epilepsy.

Acknowledgments

REFERENCES

Arikkath J, Campbell KP. Auxiliary subunits: essential components of the voltage-gated calcium channel complex. Curr. Opin. Neurobiol. 2003; 13:298–307. [PubMed: 12850214]

Arikkath J, Felix R, Ahern C, Chen CC, Mori Y, Song I, Shin HS, Coronado R, Campbell KP. Molecular characterization of a two-domain form of the neuronal voltage-gated P/Q-type calcium channel alpha(1)2.1 subunit. FEBS Lett. 2002; 532:300–308. [PubMed: 12482583]

Barrett CF, Cao YQ, Tsien RW. Gating deficiency in a familial hemiplegic migraine type 1 mutant P/Q-type calcium channel. J Biol Chem. 2005; 280:24064–24071. [PubMed: 15795222]

Battistini S, Stenirri S, Piatti M, Gelfi C, Righetti PG, Rocchi R, Giannini F, Battistini N, Guazzi GC, Ferrari M, Carrera P. A new CACNA1A gene mutation in acetazolaminde-responsive familial hemiplegic migraine and ataxia. Neurology. 1999; 53:38–43. [PubMed: 10408534]

Berrow NS, Campbell V, Fitzgerald EM, Brickley K, Dolphin AC. Antisense depletion of beta-subunits modulates the biophysical and pharmacological properties of neuronal calcium channels. J. Physiol. 1995; 482:481–491. [PubMed: 7537818]

Bichet D, Veronique C, Sandrine G, Carlier E, Volsen S, Hoshi T, Mori Y, De Waard M. The I–II loop of the calcium channel alpha1 subunit contains an endoplasmic reticulum retention signal antagonized by the beta subunit. Neuron. 2000; 25:177–190. [PubMed: 10707982]

Brice NL, Dolphin AC. Differential plasma membrane targeting of voltage-dependent calcium channel subunits expressed in a polarized epithelial cell line. Physiol. 1999; 515:685–694.

Brice NL, Berrow NS, Campbell V, Page KM, Brickley K, Tedder I, Dolphin AC. Importance of the different beta subunits in the membrane expression of the alpha1A and alpha2 calcium channel subunits: studies using a depolarization-sensitive alpha1A antibody. Eur J Neurosci. 1997; 9:749–759. [PubMed: 9153581]

Canti C, Davies A, Berrow NS, Butcher AJ, Page KM, Dolphin AC. Evidence for two concentration-dependent processes for beta-subunit effects on alpha1B calcium channels. Biopys. J. 2001; 81:1439–1451.

Cao YQ, Tsien RW. Effects of familial hemiplegic migraine type 1 mutations on neuronal P/Q-type Ca2+ channel activity and inhibitory synaptic transmission. Proc. Natl. Acad. Sci. USA. 2005; 102:2590–2595. [PubMed: 15699344]

Cao YQ, Piedras-Renteria ES, Smith GB, Chen G, Harata NC, Tsien RW. Presynaptic Ca2+ channels compete for channel type-preferring slots in altered neurotransmission arising from Ca2+ channelopathy. Neuron. 2005; 43:387–400. [PubMed: 15294146]

Catterall WA, Perez-Reyes E, Snutch TP, Striessnig J. International Union of Pharmacology. XLVIII. Nomenclature and structure-function relationships of voltage-gated calcium channels. Pharmacol. Rev. 2005; 57:411–425. [PubMed: 16382099]

Cornet V, Bichet D, Sandoz G, Marty I, Brocard J, Bourinet E, Mori Y, Villaz M, De Waard M. Multiple determinants in voltage-dependent P/Q calcium channels control their retention in the endoplasmic reticulum. Eur. J. Neurosci. 2002; 16:883–895. [PubMed: 12372025]

Cuchillo-Ibanez I, Aldea M, Brocard J, Albillos A, Weiss N, Garcia AG, De Waard M. Inhibition of voltage-gated calcium channels by sequestration of beta subunits. Biochem. Biophys. Res. Commun. 2003; 311:1000–1007. [PubMed: 14623281]

De Waard M, VES S, Pragnell M, Campbell KP. Identification of critical amino acids involved in alpha-beta interaction in voltage dependent Ca2+ channels. FEBS Lett. 1996; 380

Denier C, Ducros A, Durr A, Eymard B, Chassande B, Tournier-Lasserve E. Missense CACNA1A mutation causing episodic ataxia type 2. Arch. Neurol. 2001; 58:292–295. [PubMed: 11176968]

Denier C, Ducros A, Vahedi K, Joutel A, Thierry P, Ritz A, Castelnovo G, Deonna T, Gerard P, Devoize JL, Gayou A, Perrouty B, Soisson T, Autret A, Warter JM, Vighetto A, Van Bogaert P, Alamowitch S, Roullet E, Tournier-Lasserve E. High prevalence of CACNA1A truncations and broader clinical spectrum in episodic ataxia type 2. Neurology. 1999; 52:1816–1821. [PubMed: 10371528]

Ertel EA, Campbell KP, Harpold MM, Hofmann F, Mori Y, Perez-Reyes E, Schwartz A, Snutch TP, Tanabe T, Birnbaumer L, Tsien RW, Catterall WA. Nomenclature of voltage-gated calcium channels. Neuron. 2000; 25:533–535. [PubMed: 10774722]

Eunson LH, Graves TD, Hanna MG. New calcium channel mutations predict aberrant RNA splicing in episodic ataxia. Neurology. 2005; 65:308–310. [PubMed: 16043807]

Gao T, Chien AJ, Hosey MM. Complexes of the alpha1C and beta subunits generate the necessary signal for membrane targeting of class C L-type calcium channels. J. Biol. Chem. 1999; 274:2137–2144. [PubMed: 9890976]

Guida S, Trettel F, Pagnutti S, Mantuano E, Tottene A, Veneziano L, Fellin T, Spadaro M, Stauderman K, Williams M, Volsen S, Ophoff R, Frants R, Jodice C, Frontali M, Pietrobon D. Complete loss of P/Q calcium channel activity caused by CACNA1A missense mutation carried by patients with episodic ataxia type 2. AmJ. Hum. Genet. 2001; 68:759–764.

Imbrici P, Eunson LH, Graves TD, Bhatia KP, Wadia NH, Kullmann DM, Hanna MG. Late-onset episodic ataxia type 2 due to an in-frame insertion in CACNA1A. Neurology. 2005; 65:944–946. [PubMed: 16186543]

Imbrici P, Jaffe SL, Eunson LH, Davies NP, Herd C, Robertson R, Kullmann DM, Hanna MG. Dysfunction of the brain calcium channel CaV2.1 in absence epilepsy and episodic ataxia. Brain. 2004; 127:2682–2692. [PubMed: 15483044]

Jen J. Calcium channelopathies in the central nervous system. Curr Opin Neurobiol. 1999; 9:274–280. [PubMed: 10395579]

Jen J. Familial Episodic Ataxias and Related Ion Channel Disorders. Curr Treat Options Neurol. 2000; 2:429–431. [PubMed: 11096768]

Jen J, Kim GW, Baloh RW. Clinical Spectrum of episodic ataxia type 2. Neurology. 2004; 62:17–22. [PubMed: 14718690]

Jen J, Yue Q, Nelson SF, Yu H, Litt M, Nutt J, Baloh RW. A novel nonsense mutation in CACNA1A causes episodic ataxia and hemiplegia. Neurology. 1999; 53:34–37. [PubMed: 10408533]

Jen J, Wan J, Graves M, Yu H, Mock AF, Coulin CJ, Kim G, Yue Q, Papazian DM, Baloh RW. Loss-of-function EA2 mutations are associated with impaired neuromuscular transmission. Neurology. 2001; 57:1843–1848. [PubMed: 11723274]

Jeng CJ, Chen YT, Chen YW, Tang CY. Dominant-Negative Effects of Human P/Q-type Ca2+ Channel Mutations Associated with Episodic Ataxia Type 2. Am. J. Physiol. Cell Physiol. 2006; 290:1209–1220.

Jouvenceau A, Eunson LH, Spauschus A, Ramesh V, Zuberi SM, Kullmann DM, Hanna MG. Human epilepsy associated with dysfunction of the brain P/Q-type calcium channel. Lancet. 2001; 358:801–807. [PubMed: 11564488]

Kordasiewicz HB, Thompson RM, Clark HB, Gomez CM. Carboxyl termini of P/Q-type Ca2+ channel {alpha}1A subunits translocate to nuclei and promote polyglutamine-mediated toxicity. Hum. Mol. Genet. 2006; 15:1587–1599. [PubMed: 16595610]

Lacerda AE, Kim HS, Ruth P, Perez-Reyes E, Flockerzi V, Hofmann F, Birnbaumer L, Brown AM. Normalization of current kinetics by interaction between the alpha 1 and beta subunits of the skeletal muscle dihydropyridine-sensitive Ca2+ channel. Nature. 1991; 352:527–530. [PubMed: 1650913]

Maltez JM, Nunziato DA, Kim J, Pitt GS. Essential Ca(V)beta modulatory properties are AID-independent. Nat. Struct. Mol. Biol. 2005; 12:372–377. [PubMed: 15750602]

Mantuano E, Veneziano L, Spadaro M, Giunti P, Guida S, MG L, Verriello L, Wood N, Jodice C, Frontali M. Clusters of non-truncating mutations of P/Q type Ca2+ channel subunit Ca(v)2.1 causing episodic ataxia 2. J. Med. Genet. 2004; 41:1–6. [PubMed: 14729816]

Martin-Moutot N, Charvin N, Leveque C, Satom K, Nishiki T, Kozaki S, Takahashi M, Seagar M. Interaction of SNARE complexes with P/Q-type calcium channels in rat cerebellar synaptosomes. J. Biol. Chem. 1996; 271:6567–6570. [PubMed: 8636067]

Mochida S, Sheng ZH, Baker C, Kobayashi H, Catterall WA. Inhibition of neurotransmission by peptides containing the synaptic protein interaction site of N-type Ca2+ channels. Neuron. 1996; 17:781–788. [PubMed: 8893034]

Mochida S, Westenbroek RE, Yokoyama CT, Itoh K, Catterall WA. Subtype-selective reconstitution of synaptic transmission in sympathetic ganglion neurons by expression of exogenous calcium channels. Proc. Natl. Acad. Sci. USA. 2003a; 100:2813–2818. [PubMed: 12601155]

Mochida S, Westenbroek RE, Yokoyama CT, Zhong H, Myers SJ, Scheuer T, Itoh K, Catterall WA. Requirement for the synaptic protein interaction site for reconstitution of synaptic transmission by

P/Q-type calcium channels. Proc. Natl. Acad. Sci. USA. 2003b; 100:2819–2824. [PubMed: 12601156]

Ophoff RA, Terwindt GM, Vergouwe MN, van Eijk R, Oefner PJ, Hoffman SM, Lamerdin JE, Mohrenweiser HW, Bulman DE, Ferrari M, Haan J, Lindhout D, van Ommen GJ, Hofker MH, Ferrari MD, Frants RR. Familial hemiplegic migraine and episodic ataxia type-2 are caused by mutations in the Ca2+ channel gene CACNL1A4. Cell. 1996; 87:543–552. [PubMed: 8898206]

Page KM, Heblich F, Davies A, Butcher AJ, Leroy J, Bertaso F, Pratt WS, Dolphin AC. Dominant-negative calcium channel suppression by truncated constructs involves a kinase implicated in the unfolded protein response. J. Neurosci. 2004; 24:5400–5409. [PubMed: 15190113]

Piedras-Renteria ES, Watase K, Harata N, Zhuchenko O, Zoghbi HY, Lee CC, Tsien RW. Increased expression of alpha 1A Ca2+ channel currents arising from expanded trinucleotide repeats in spinocerebellar ataxia type 6. J. Neurosci. 2001; 21:9185–9193. [PubMed: 11717352]

Pragnell M, De Waard M, Mori Y, Tanabe T, Snutch TP, Campbell KP. Calcium channel beta-subunit binds to a conserved motif in the I–II cytoplasmic linker of the alpha 1-subunit. Nature. 1994; 368:67–70. [PubMed: 7509046]

Ptacek LJ. The place of migraine as a channelopathy. Curr Opin Neurol. 1998; 11:217–226. [PubMed: 9642539]

Ptacek LJ. Ion channel diseases: episodic disorders of the nervous system. Semin Neurol. 1999; 19:363–369. [PubMed: 10716659]

Raghib A, Bertaso F, Davies A, Page KM, Meir A, Bogdanov Y, Dolphin AC. Dominant-negative suppression of voltage-gated calcium channel Cav2.2 induced by truncated constructs. J Neurosci. 2001; 21:8495–8504. [PubMed: 11606638]

Restituito S, Thompson R, Eliet J, Raike R, Riedle M, Charnet P, Gomez CM. The polyglutamine expansion in spinocerebellar ataxia type 6 causes a beta subunit-specific enhanced activation of P/Q-type calcium channels in Xenopus oocytes. J. Neurosci. 2000; 20:6394–6403. [PubMed: 10964945]

Rock, DM.; Horne, WA.; Stoehr, SJ.; Hashimoto, C.; Zhou, M.; Cong, R.; Palma, A.; Hidayetoglu, D.; Offord, J. Does alpha1E code for T-type calcium channels? A comparison of recombinant alpha1E calcium channels with GH3 pituitary T-type and recombinant alpha1B calcium channels. In: Tsien, RW.; Clozel, JP.; Nargeot, J., editors. Low-voltage-activated T-type calcium channels. Adis International; 1989. p. 279-289.

Scoggan KA, Friedman JH, Bulman DE. CACNA1A mutation in a EA-2 patient responsive to acetazolamide and valproic acid. CanJ. Neurol. Sci. 2006; 33:68–72.

Singer D, Biel M, Lotan I, Flockerzi V, Hofmann F, Dascal N. The roles of the subunits in the function of the calcium channel. Science. 1991; 253:1553–1557. [PubMed: 1716787]

Spacey SD, Materek LA, Szczygielski BI, Bird TD. Two novel CACNA1A gene mutations associated with episodic ataxia type 2 and interictal dystonia. Arch. Neurol. 2005; 62:314–316. [PubMed: 15710862]

Spacey SD, Hildebrand ME, Materek LA, Bird TD, Snutch TP. Functional implications of a novel EA2 mutation in the P/Q-type calcium channel. Ann. Neurol. 2004; 56:213–220. [PubMed: 15293273]

Stea A, Tomlinson WJ, Soong TW, Bourinet E, Dubel SJ, Vincent SR, Snutch TP. Localization and functional properties of a rat brain alpha 1A calcium channel reflect similarities to neuronal Q- and P-type channels. Proc. Natl. Acad. Sci. USA. 1994; 91:10576–10580. [PubMed: 7524096]

Subramony SH, Schott K, Raike RS, Callahan J, Langford LR, Christova PS, Anderson JH, Gomez CM. Novel CACNA1A mutation causes febrile episodic ataxia with interictal cerebellar deficits. Annal. Neurol. 2003; 54:725–731. [PubMed: 14681882]

Swensen AM, Bean BP. Ionic mechanisms of burst firing in dissociated Purkinje neurons. J. Neurosci. 2003; 23:9650–9663. [PubMed: 14573545]

Usowicz MM, Sugimori M, Cherksey B, Llinas R. P-type calcium channels in the somata and dendrites of adult cerebellar Purkinje cells. Neuron. 1992; 9:1185–1199. [PubMed: 1281419]

van den Maagdenberg AM, Kors EE, Brunt ER, van Paesschen W, Pascual J, Ravine D, Keeling S, Vanmolkot KR, Vermeulen FL, Terwindt GM, Haan J, Frants RR, Ferrari MD. Episodic ataxia

type 2:Three novel truncating mutations and one novel missense mutation in the CACNA1A gene. J. Neurol. 2002; 249:1515–1519. [PubMed: 12420090]

Walker D, Bichet D, Campbell KP, De Waard M. A beta 4 isoform-specific interaction site in the carboxyl-terminal region of the voltage-dependent Ca2+ channel alpha 1A subunit. J. Biol. Chem. 1998; 273:2361–2367. [PubMed: 9442082]

Walker D, Bichet D, Geib S, Mori E, Cornet V, Snutch TP, Mori Y, De Waard M. A new beta subtype-specific interaction in alpha1a subunit controls P/Q-type Ca2+ channel activation. J. Biol. Chem. 1999; 274:12383–12390. [PubMed: 10212211]

Walter JT, Alvina K, Womack MD, Chevez C, Khodakhah K. Decreases in the precision of Purkinje cell pacemaking cause cerebellar dysfunction and ataxia. Nat. Neurosci. 2006; 9:389–397. [PubMed: 16474392]

Wan J, Carr JR, Baloh RW, Jen JC. Nonconsensus intronic mutations cause episodic ataxia. Ann. Neurol. 2005a; 57:131–135. [PubMed: 15622542]

Wan J, Khanna R, Sandusky M, Papazian DM, Jen JC, Baloh RW. CACNA1A mutations causing episodic and progressive ataxia alter channel trafficking and kinetics. Neurology. 2005b; 64:2090–2097. [PubMed: 15985579]

Wappl E, Koschak A, Poteser M, Sinnegger MJ, Walter D, Eberhart A, Groschner K, Glossmann H, Kraus RL, Grabner M, Striessnig J. Functional consequences of P/Q-type Ca2+ channel Cav2.1 missense mutations associated with episodic ataxia type 2 and progressive ataxia. J. Biol. Chem. 2002; 277:6960–6966. [PubMed: 11742003]

Westenbroek RE, Sakurai T, Elliott EM, Hell JW, Starr TV, Snutch TP, Catterall WA. Immunochemical identification and subcellular distribution of the alpha 1A subunits of brain calcium channels. J. Neurosci. 1995; 15:6403–6418. [PubMed: 7472404]

Wittemann S, Mark MD, Rettig J, Herlitze S. Synaptic localization and presynaptic function of calcium channel beta 4-subunits in cultured hippocampal neurons. J. Biol. Chem. 275:37807–37814. 200. [PubMed: 10931840]

Womack MD, Khodakhah K. Dendritic control of spontaneous bursting in cerebellar Purkinje cells. J. Neurosci. 2004; 24:3511–3521. [PubMed: 15071098]

Yue Q, Jen JC, Thwe MM, Nelson SF, Baloh RW. De novo mutation in CACNA1A caused acetazolamide-responsive episodic ataxia. Am. J. Med. Genet. 1998; 77:298–301. [PubMed: 9600739]
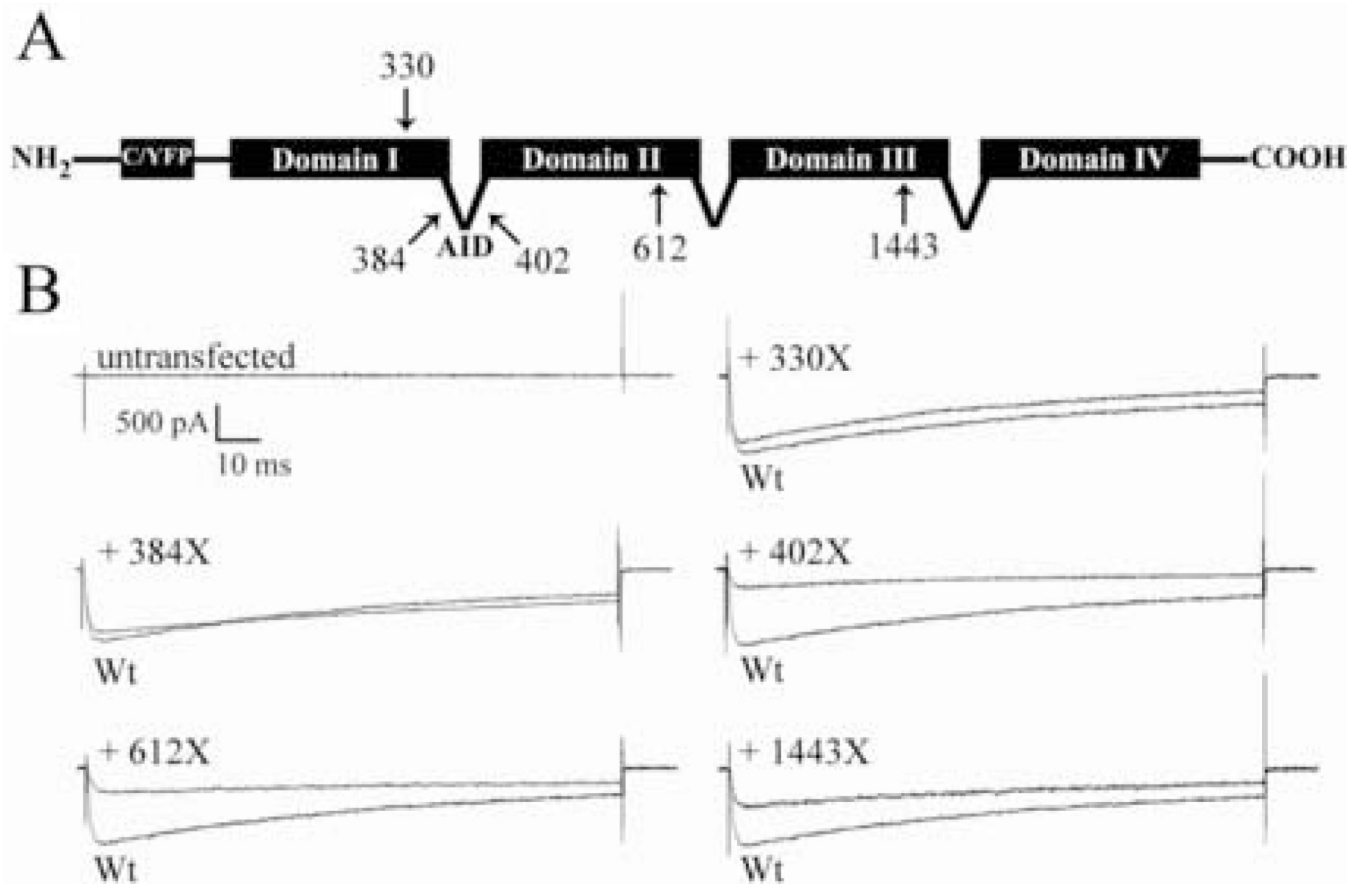
Figure 1. Design and co-expression of CFP-tagged wild-type $\alpha_1$2.1 subunits with YFP-tagged truncations

A. Schematic of CFP-tagged wild-type $\alpha_1$2.1 subunits (Wt) and YFP-tagged truncations indicates the amino-acid residue numbers and approximate length of each truncated isoform. The alpha interaction domain, AID, between repeat domains I and II is also marked. **B**. Current traces depicted were elicited with 0 mV depolarizing pulses from −80 mV holding potentials following transient co-expression of truncations with Wt subunits in β_1-HEK cells. Traces from cells co-expressing truncations with Wt subunits are overlaid with those obtained from control cells expressing Wt subunits alone.
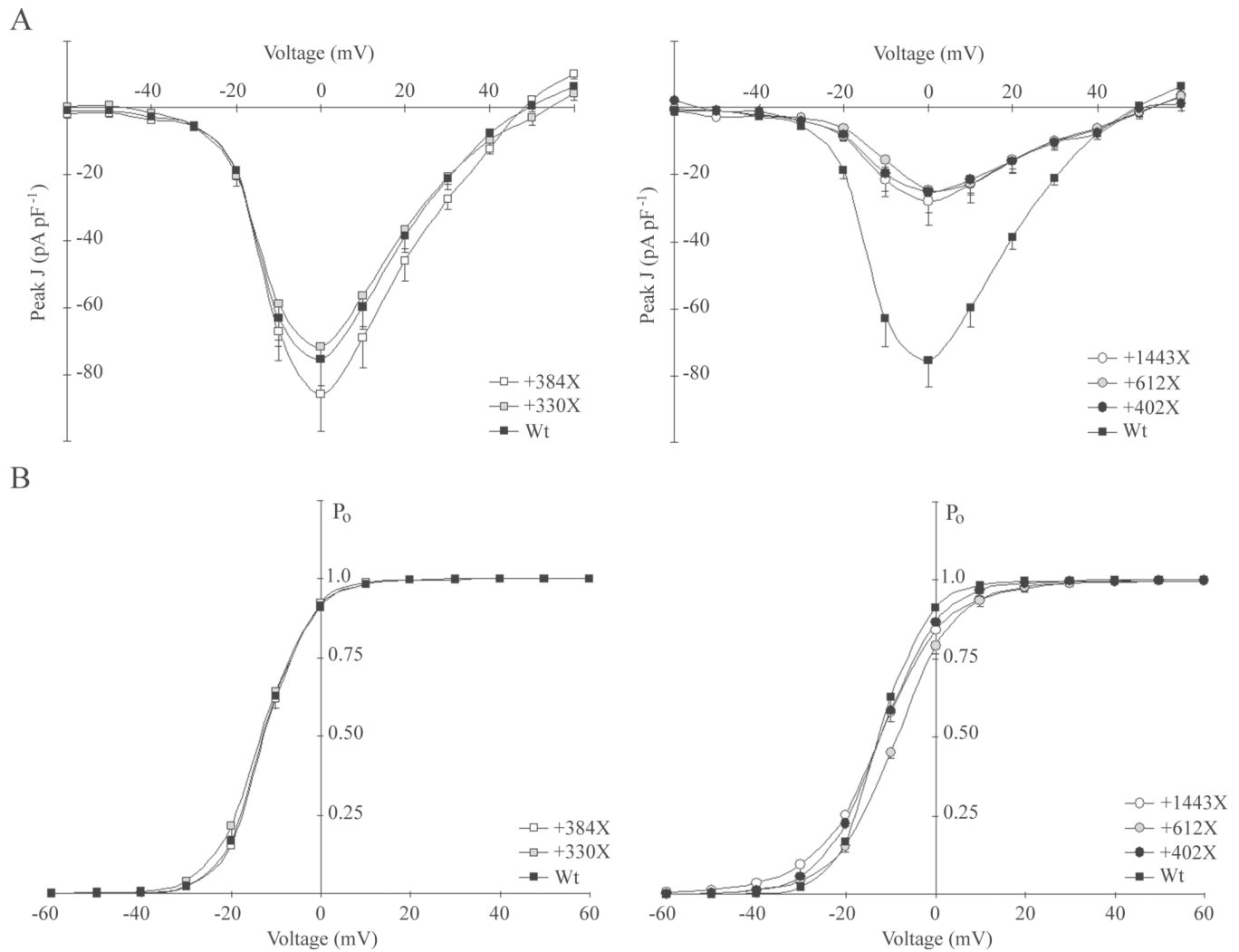
A

B

Figure 2. Whole-cell Ca$_v$2.1 currents from β1-HEK cells co-expressing α$_1$2.1 truncations with wild-type subunits

Whole-cell currents were elicited with 150 ms step pulses from −60 to +60 mV at intervals of 10 seconds from a hold of −80 mV. **A**. Mean peak current density responses (Peak J, pA pF^{-1}) plotted against voltage steps (mV) with error bars representing SEM. Current-voltage plots of recordings from cells co-expressing CFP-tagged wild-type α$_1$2.1 subunits (Wt) and YFP-tagged truncations terminating proximal to the AID are similar in magnitude to control recordings from control cells expressing Wt subunits alone (Left panel). Current-voltage plots of recordings from cells co-expressing α$_1$2.1 truncations terminating distal to the AID reveal severely reduced current densities across all voltages compared to control cells (Right panel). **B**. Whole-cell current data for individual cells were fitted with the modified Boltzmann equation: Peak J = G (V−V$_{rev}$)[1 + exp(V$_{0.5}$−V)$^{−k}$]$^{−1}$ to compare Ca$_v$2.1 channel open probability (P$_o$) across all voltage steps. The mean of each group is expressed with error bars representing SEM. Compared to currents from control cells expressing Wt subunits alone, those from cells co-expressing truncations terminating proximal to the AID in most cases exhibited normal P$_o$ profile across all voltages (Left panel). Most of the P$_o$ profiles of currents from cells co-expressing truncations terminating distal to the AID reveal minor deviations from control, except for currents from cells co-expressing YFP-612X truncations, which appeared to activate at more positive voltages.
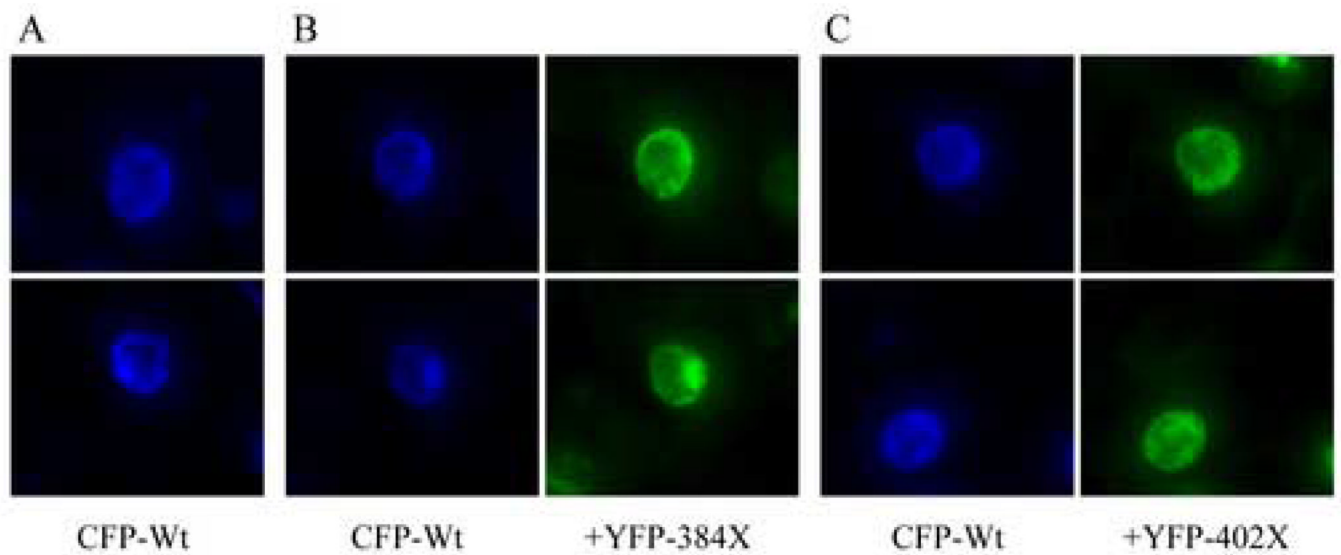
Figure 3. Expression patterns of CFP-tagged wild-type $\alpha_1$2.1 subunits and YFP-tagged truncations co-expressed in β1-HEK cells
Representative epifluorescence images from cells treated identically to those used for electrophysiological analyses. **A.** Transfecting β1-HEK cells with CFP-tagged wild-type $\alpha_1$2.1 subunit cDNA constructs (CFP-Wt) resulted in an abundance of cells with CFP fluorescence distributed in patterns suggesting robust membrane expression. **B. and C**. Compared to control cells expressing CFP-Wt subunits alone, no changes were discernable to the levels or patterns of CFP fluorescence in cells co-expressing YFP-tagged truncations terminating proximal (YFP-384X) or distal (YFP-402X) to the AID.
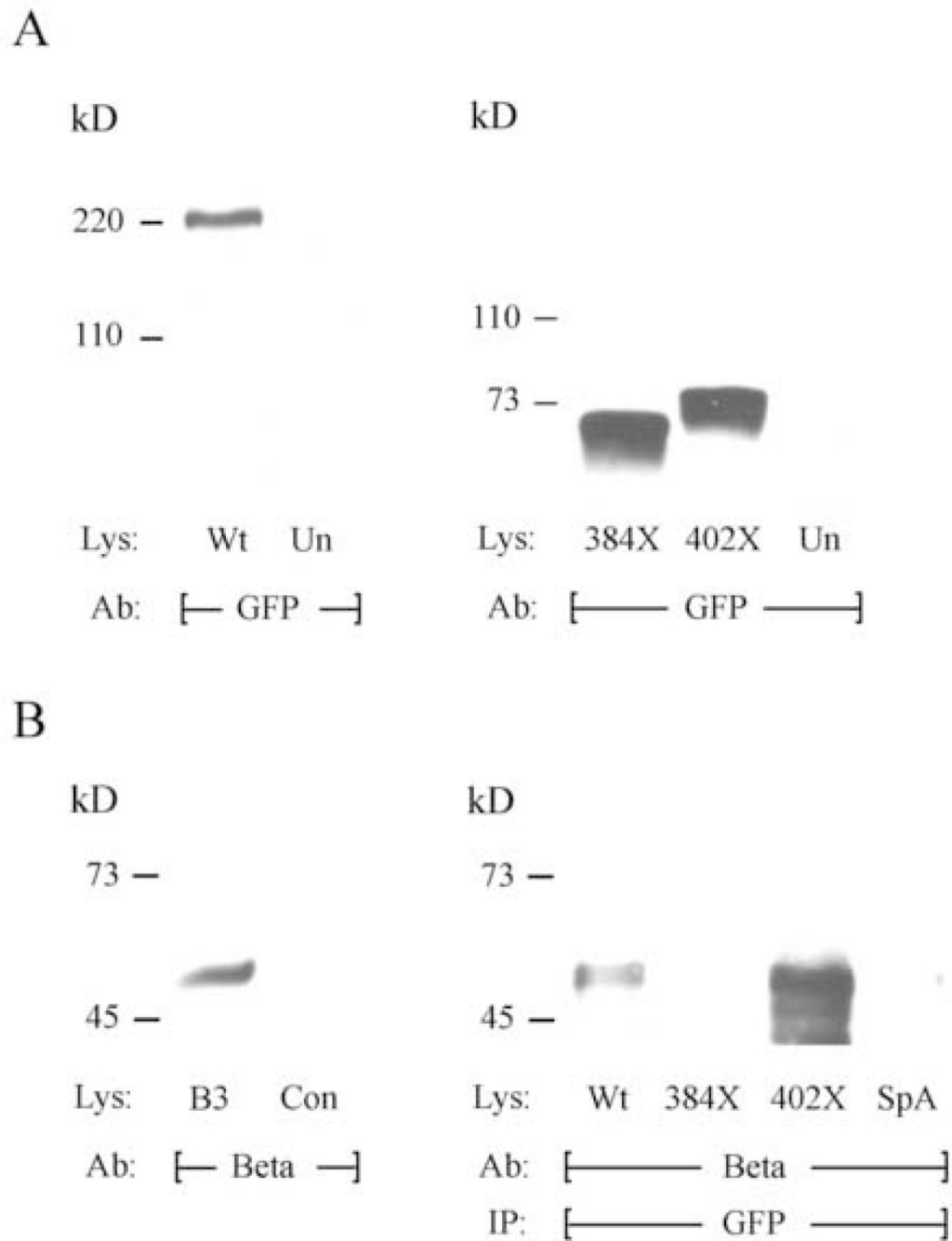
Figure 4. Truncation proximal to the AID prevents $\alpha_1$2.1-β subunit interactions
A. Western blotting lysates (Lys) from β3-HEK cells with GFP antibody (Ab) detects the predicted $\alpha_1$2.1 isoforms in cells expressing CFP-tagged wild-type $\alpha_1$2.1 subunits (Wt) or YFP-tagged 384X or 402X truncations, but GFP Ab does not react with lysates from untransfected (Un) β3-HEK cells. **B**. Western blotting with β3 Ab (Beta) detects an approximate 60 kD β3 subunit species in lysates from β3-HEK cells (B3) but not control (Con) HEK cells (left panel). Western blotting with β3 Ab following immunoprecipitation (IP) of lysates with GFP Ab detects the same β3 subunit species in preparations from β3-HEK cells expressing CFP-tagged wild-type $\alpha_1$2.1 subunits or YFP-tagged 402X truncations

but not from cells expressing 384X truncations, which terminate proximal to the AID (right panel).

Table 1

$Ca_v2.1$ currents from β_1-HEK cells co-expressing $\alpha_12.1$ truncations and wild-type subunits

	Wild type	+ 330X	+ 384X	+ 402X	+ 612X	+ 1443X
J_{peak} (pA pF^{-1})	-75.5 ± 7.9 (16)	-71.8 ± 12.8 (13)	-85.8 ± 11.2 (7)	-25.2 ± 5.9^b (7)	-24.5 ± 3.9^c (12)	-27.8 ± 7.1^b (9)
C_m (pF)	11.7 ± 0.6	9.2 ± 1.0	10.2 ± 1.0	12.1 ± 1.8	11.6 ± 0.8	11.5 ± 1.5
G (pA pF^{-1} mV^{-1})	2.0 ± 0.2	1.8 ± 0.3	2.0 ± 0.3	0.5 ± 0.1^b	0.7 ± 0.1^c	0.7 ± 0.2^b
$V_{0.5}$ (mV)	-12.2 ± 0.8	-13.0 ± 1.0	-12.1 ± 0.7	-11.6 ± 0.6	-8.6 ± 0.7^a	-12.2 ± 1.1
k (mV)	4.6 ± 0.3	5.0 ± 0.4	4.7 ± 0.3	7.7 ± 1.1	6.8 ± 0.6^a	6.3 ± 0.3^c
I_{peak} (ms)	6.3 ± 0.3 (11)	5.8 ± 0.4 (7)	6.7 ± 0.3 (7)	7.0 ± 0.8 (6)	7.3 ± 0.5 (11)	7.3 ± 0.5 (8)
I_r50 (%)	59.4 ± 2.4	52.6 ± 7.6	70.0 ± 1.9	56.1 ± 4.1	66.6 ± 2.6	53.8 ± 2.9

Data are expressed as means ± SEM and tested for significance using ANOVA and *post hoc* Bonferroni correction. Jpeak measured at 0 mV step pulse; Ipeak and I$_r$50 measured at 0, 10 and 20 mV step pulses. (N) = number of cells for current density or kinetic measurements. Kinetic measurements are from recordings of cells that survived throughout the experiment and expressed detectable levels of $Ca_v2.1$ currents.

$p^a < 0.005$,

$p^b < 0.001$,

$p^c < 0.0001$.

Table 2

Expression levels of $\alpha_1 2.1$ truncations and wild-type subunits co-expressed in β_1-HEK cells

	Wt	+ 384X	+ 402X	+ 612X	+ 1443X
Cyan RF	50.1 ± 3.8 (27)	52.0 ± 3.0 (33)	50.3 ± 4.7 (18)	48.4 ± 6.9 (20)	69.2 ± 5.8^a (17)
Yellow RF	NA	82.9 ± 7.0	43.0 ± 4.9^b	81.7 ± 12.5	66.0 ± 6.5
C:Y Ratio	NA	0.86 ± 0.12	1.4 ± 0.17^a	0.74 ± 0.11	1.17 ± 0.10

Data are expressed as means ± SEM and tested for significance using ANOVA and *post hoc* Bonferrroni correction. Conditions were identical to those for physiological experiments. All values calculated for individual cells and then averaged across groups. RF = background-subtracted relative fluorescence levels. (N) = number of cells, C:Y Ratio = ratio of Cyan and Yellow RF levels,

$p^a < 0.005$,

$p^b < 0.001$